Prepared for submission to JCAP

A luminosity constraint on the dark matter origin of Fermi unassociated sources

Y. Amoura,[a,b,1] **J. M. Siegal-Gaskins,**[c] **F. Massaro** [d,2]

[a]université Pierre et Marie Curie,
Paris,75005 France
[b]ENS Cachan,
Cachan, 94230 France
[c]Grappa, Institue of Physics, University of Amsterdam
1098 XH Amsterdam, Netherlands

E-mail: yuba.amoura@etu.upmc.fr, jgaskins@uva.nl, third@one.univ

Abstract. In this paper we perform a study of the unassociated sources of the catalogs of the Fermi Large Area Telescope assuming their origin is Dark Matter...

[1]note.
[2]Also at Some University.

Contents

1 Introduction

The Fermi Large Area Telescope has been lunched 5 years ago and provide us by more than 3000 high energy sources, among which 1010 remain unassociated whith any conterpart at lower energies[1], a part of these sources may be unidentified blazers, pulsars and other gamma-ray emitting astrophyisical objects, however, a Dark Matter(DM) origin of the signal should not be excluded. [2]

Numerical simulations predict hierarchical structure of dark matter,[3]... small subhalos merging to bigger ones and form hosting galactic halos, this predicts a very large number of subhalos in galactic halos like the milky way's, these subhalos may eventually be detected as gamma-ray sources, the bigger ones can be identified as the milky way satellite galaxies such as the Large and Small Magelan Cloud howewer, it is much harder to identify the smaller

subhalos which could be among some of the unassociated sources of Fermi catalog. Then, the question that rises up is whether some of these sources can be DM subhalos, if yes how many of them could be ?

We will follow the idea developped in [4] where they used Fermi's predecessor EGRET, and use M31's luminosity to put a constraint on the origin of the unidentified sources of EGRET. Fermi has detected many more sources with detailed informations (Variability, localisation, Spectrum...), these informations may help us to distinguish between good DM subhalos candidates and what would more likely be an astrophysical source.

We will consider that M31 and the milky way have nearly the same gamma-ray and dark matter properties,(a paper for that ?) and use a model of M31 as a luminosity reference to get a constraint on the Fermi unassociated sources. we simulate a realistic Dark Matter subhalos population using these sources and calculate the resulting luminosity, and then compare it to M31 luminosity, the overshooting of this value would mean that the subhalos used for our simulations cannot all be dark matter subhalos. that will provide us a constraint on them.

In this paper we first look at some properties of the sources from the different fermi catalogs that we use sec 2 such as the variability, the spectrum and the angular distribution, then we discuss about the density profile we choose to implement for our simulation of the dark matter subhalos population and also for the astrophyisical component of the galaxy in sec 3, in sec 4 we look at the M31 model in particular its size and the part of the astrophysical emission. We describe the different analysis we did 5 and present the results in 6, we discuss about them, the limitations and the possible improvement in 7 and finally conclude in 8

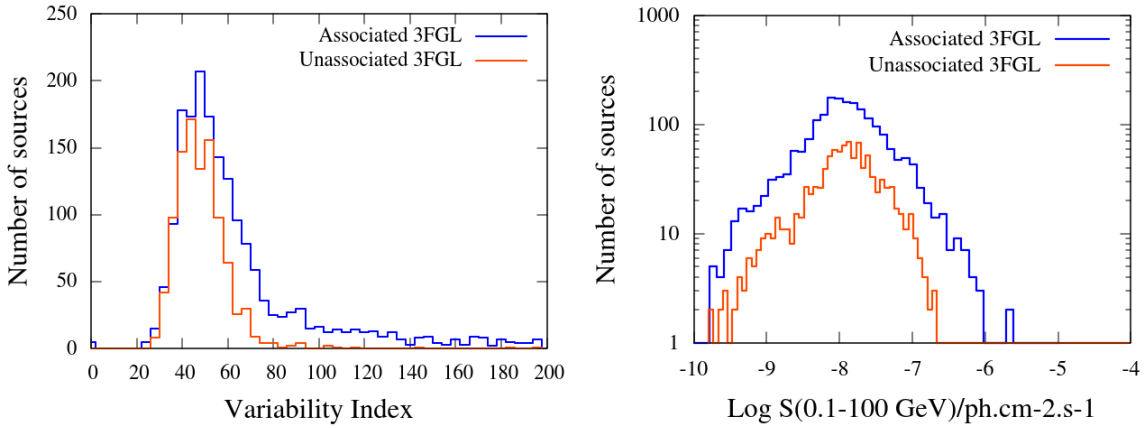

Figure 1. Left panel: variability distribution, comparison between the unassociated sources of the 3FGL catalog (orange) and the associated ones (blue), the unassociated source variability is less extended because variable sources are easier to associate. Right panel: the log S-log N diagram for the associated(blue) and unassociated(orange) sources, again the unassociated source flux is more extended, the very bright sources are easily associated. the lower flux limit corresponds to Fermi detection threeshold

2 The catalogs

We used in this work two catalogs, the Third Fermi-LAT point source catalog (3FGL) [1] and a refined catalog from both the 1FGL and 2FGL [5] where we cut every source that have a good low energy counterpart...

2.1 3FGL Catalog

The third Fermi Large Area Telescope source catalog is the latest catalog from Fermi at the time of the publication(check if it still true), the catalog contains 3034 sources, most of them are active galaxies and blazers. Pulsars represent the largest part of the galactic sources. Among all this sources, 1010 remain unassociated with any low energy counterpart, hence represent an ideal target for dark matter research...

2.1.1 Variability

In order to perform a more precise study, we need to select a good sample of possible candidates, we first look at the sources variability, represented by the *Variability Index* in the catalog since we do not expect DM subhalos to be variable. The left frame of Fig. 1 shows a comparison between the variability distribution of the unassociated and associated sources of the 3FGL catalog, most of sources with large variability index values are associated, variability is a signature of a certain type of sources such as Pulsars and is used to identify sources. A source is considered very likely variable if its Variability Index is higher than 72.44, we decided to simply take this value as a cut for our sample and consider only lower Variability Index sources, which reduce our sample from the initial 1010 unassociated sources to 983 which we consider as non variable.

2.1.2 Flux

The right frame of 1 shows the logS-logN diagram in the 0.1-100GeV energy range for both the associated and unassociated 3FGL catalog sources, the lower limit $10^{-10} ph.cm^{-2}s^{-1}$ represent the Fermi flux threshold, one can also see that the flux of associated sources is more extended than the unassociated ones, the very bright sources are easily identifiable that explains why we do not have unassociated sources at large flux...

2.1.3 Spectrum

The sources spectrum shape is devided in 3 types: a power-law with an exponontial cut-off for Pulsars with a signifanctly curved spectra, a log-normal shape (log-parabola) for all significantly curved spectra and a simple power-law for all the others, the equations are respectively:

$$\frac{dN}{dE} = K \left(\frac{E}{E_0}\right)^{-\alpha-\beta log(E/E_0)} \tag{2.1}$$

where K, E_0, α , and β are respectively the flux density, the pivot energy, the spectral index and the curvature, these parameters are given in the catalog

$$\frac{dN}{dE} = K \left(\frac{E}{E_0}\right)^{-\Gamma} \exp\left(\left(\frac{E_0}{E_c}\right)^b - \left(\frac{E}{E_c}\right)^b\right) \tag{2.2}$$

where Γ is the spectral index, E_c the energy cutoff and b the exponontial index [1]

$$\frac{dN}{dE} = K \left(\frac{E}{E_0}\right)^{-\Gamma} \tag{2.3}$$

We look more precisely at the spectral properties of the sources in 2 where we plot the spectral index distribution and compare between the unassociated and assoicated sources for

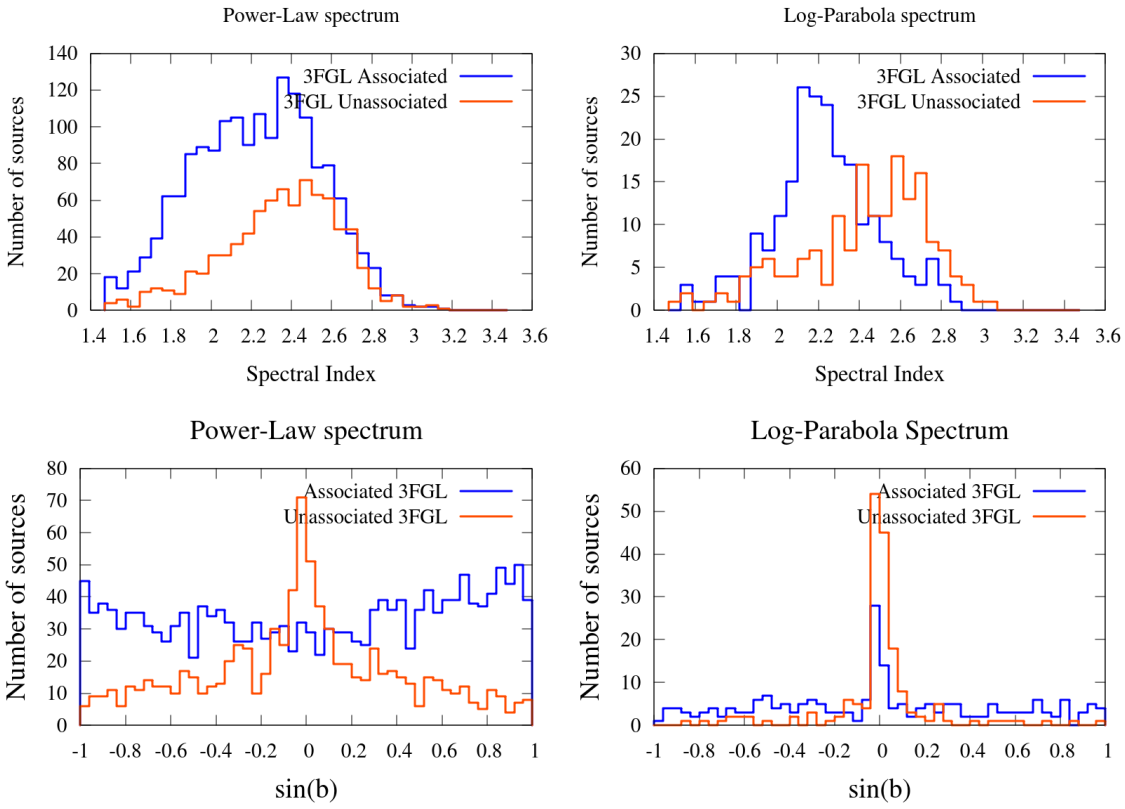

Figure 2. The spectral index and latitude distribution for the log-parabola and power-law specrum sources for the associated and the unassociated sources. Top left : the spectral index distribution for the power-low spectrum sources, where the associated and unassociated source have the same shape. Top right: the spectral index distribution for the log-parabola spectrum sources, the associated and unassociated distributions are different, which means that the proportion on different type of sources is not the same, in particular we have a larger part of galactic sources among the unassociated ones, we can see it in the bottom right panel: the latitude distribution for log-parabola spectrum sources, most of unassociated sources are in the galactic plane. And finally the latitude distribution for power-law spectrum sources on bottom left panel shows an isotropic distribution for associated sources and a bunch at low latitude for the unassociated, in fact this is due to the large background in the galactic plane that makes associations difficult

both power-law and log-parabola spectrum. For the sources with a power-law spectrum, the spectral index distribution of the associated and unassociated sources are nearly the same, while they are different for the sources that have a signifanctly curved specrta (log-parabola), this means that for the first case the unassociated are the same kind of sources that the associated ones with nearly the the same proportions, however it is highly unlikely that they are the same type of sources for the log-parabola ones, morover the latitude distribution study represented on the bottom of the 2 indicates an isotropic distribution of the power-law spectrum associated sources, which means that most of them are extra galactic ones such as different type of blazers and active galaxies. The galactic power law sources remain difficult to associated due to the high background, that explains the number of unassociated sources near the glactic plane with a power-law spectrum. however the log-parabola spectrum sources do not follow the same behavior, most of sources are at low latitudes, and we have very few

of unassociated ones at high latitudes, and a bunch near the galactic plane, the associated ones are more isotropically distributed, even if there are more at low latitudes.

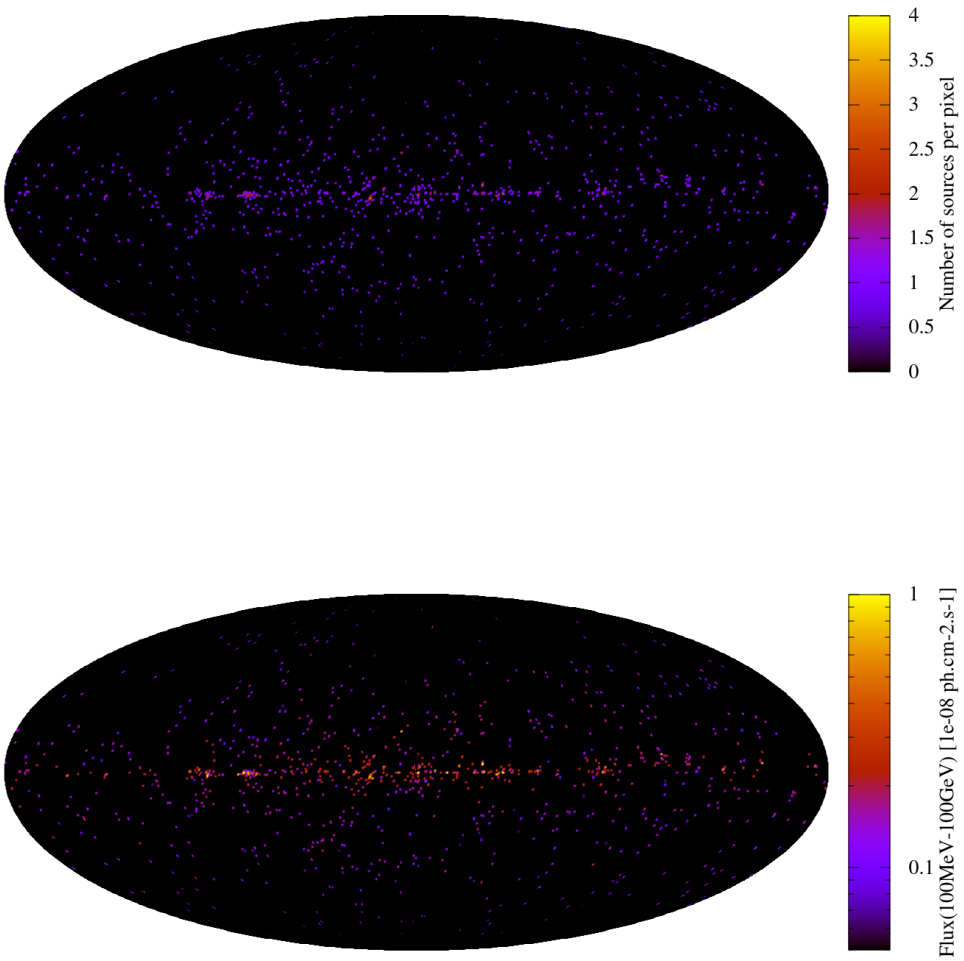

Figure 3. The distribution in the sky of the sources, on the top we have the source distribution where a pixel corresponds to 0.5°x0.5°The density of sources is large at low latitudes and isotropically distributed out of the galactic plane. on the bottom we have the flux distribution (also per pixel). the low latitude sources are much brighter, due to the large background in the galactic plane.

2.1.4 localisation

The unassociated sources sky distribution is shown on the top panel of 3, there are few very dense regions in the galactic plane, and an isotropic distribution at high latitudes, the flux distribution (bottom panel) shows an interesting feature, the sources in the galactic plane are muc brighter than the high latitude ones, probably due to the large background in the galactic plane where a source need to be very bright to overshoot the diffuse emission in the

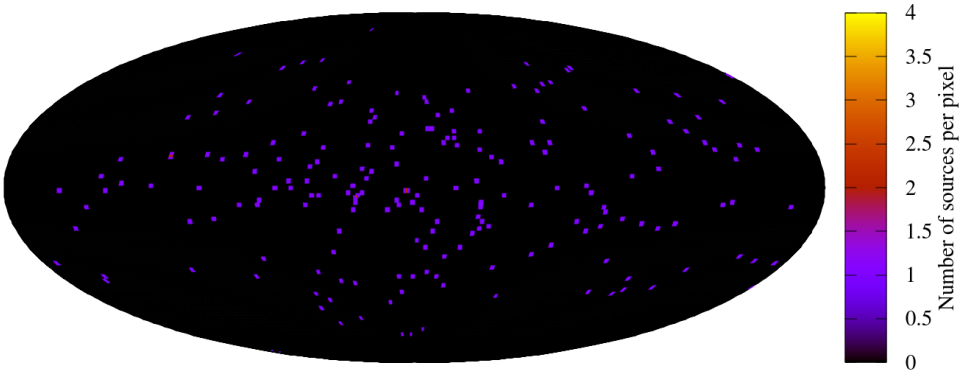

Figure 4. The sky distribution of the RA sources, which are more isotropic than the 3FGL, there are less very dense regions, the distribution corresponds more to what we could imagine for a Dark Matter subhalos population

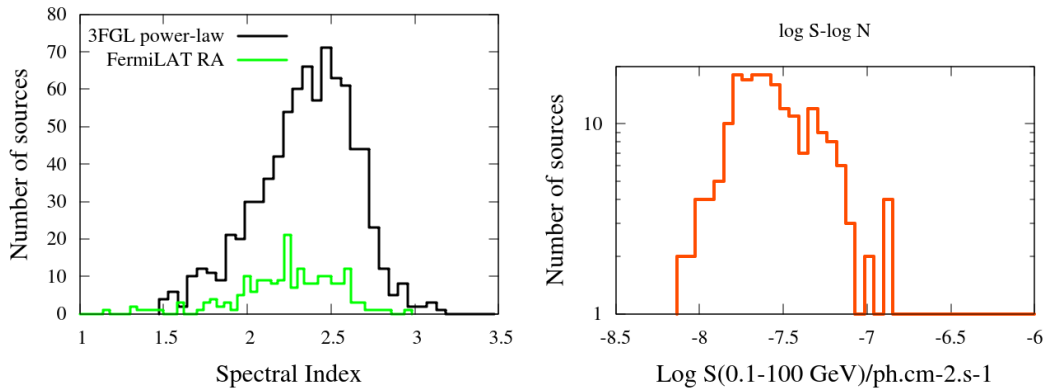

Figure 5. Left : the spectral index distribution for the the unassociated sources of both the 3FGL and RA catalogs,without a clear difference between their spectrum Right: the log S-log N diagram,one can notice a higher detection threshold 10^{-9} instead of 10^{10} for the 3FGL, which make sense,the RA catalog is an update of 1FGL and 2FGL

galaxy, an additional explanation would be simply that most of them are in the galaxy, and thus their flux is largeer than a very far blazar.

It is not surprising to find that there are more unassociated sources near the galactic plane, however we expect a population of Dark Matter subhalos to be more isotropicaly distributed, we choose for our study to consider only high latitude sources as good DM subhalos candidates, we make our cut at $10°$ and consider all sources with $b < 10°$ as an astrophysical component of the galaxy, we justify this assumption considering the very large background near the galactic plane.

2.2 FermiLAT Refined Association

The *Fermi LAT Refined Assoications* catalog (RA catalog) is an improved version of the 2FGL and 1FGL catalog made by cite(Fran et al) where they worked on associating the sources with counterparts at other wavelengths using different catalogs and different associating methods. The result is a very clean catalog where each source with a good possible candidate has been cut [5], in addition we decided to cut any source that has a possible counterpart, finally we have 195 sources left, which is less than the 983 of the 3FGL non variable unassociated sources, we will do the study using the two different catalogs and discuss about the different results.

The RA sources are distributed more isotropically in comparison with the 3FGL 4, this is more compatible with what we could expect for a DM subhalo population. we do not need to cut more sources or make any additional assuption on the origin of the sources since the catalog is already very clean.

We show some properties of the RA sources in 5, the spectral index distribution on the left panel compared with 3FGL power-law unassociated sources, the plot does not show significant difference between their spectrum... The logS-logN diagram is represented on the right panel, the lower limit is larger than the 3FGL one, the reason is simply that we use 1FGL and 2FGL sources which are previous Fermi catalogs...

3 Source distribution Profile

3.1 Dark Matter profile

The next step was to choose a good dark matter profile, our model follows the latest numerical sumulations, a large halo with sustructures,... (saying something about DM profile) (cite dm profile papers) [3] , [6] is giving a subhalo number density profile well fitted by an Einasto profile:

$$n(r) \propto e^{-\frac{2}{\alpha}[(r/r_s)^{\alpha}-1]} \tag{3.1}$$

with best fit parameters $r_s = 199kpc$ and $\alpha = 0.678$.

While [7] is giving a subhalos number destiy proportional to $\rho(r) \times r$ where their mass density profile is well fitted by a Generalised NFW profile:

$$\rho(r) = \frac{\rho_0}{(r/r_s)^{\gamma}\,(r/r_s - 1)^{3-\gamma}} \tag{3.2}$$

with best fit parameters $r_s = 28.1kpc$ and $\gamma = 1.24$

The left panel of figure 6 shows the number density profiles normalised by their mean value, for both the Einasto and GNFW profile, the shapes are different, the Einasto is flatter at small radius and falls very fast at large ones where the GNFW is more extended. Rhe right panel shows the radial distribution of sources, against the distance from the galactic center, what we can see is that for both profiles most of sources are in the outer regions of the halo, (>100) and they do not fall before 300kpc, it is even worst for the GNFW profile where the number of sources does not stop increasing with radius. That makes importent the size of the DM Halo of our model, considering a halo with a 100kpc maximum radius will give a completely different luminosity than considering a 300kpc radius halo. we took 250 as a realistic size for the dark matter halo of the milky way, and we used the Einasto profile which gives more conservative results.

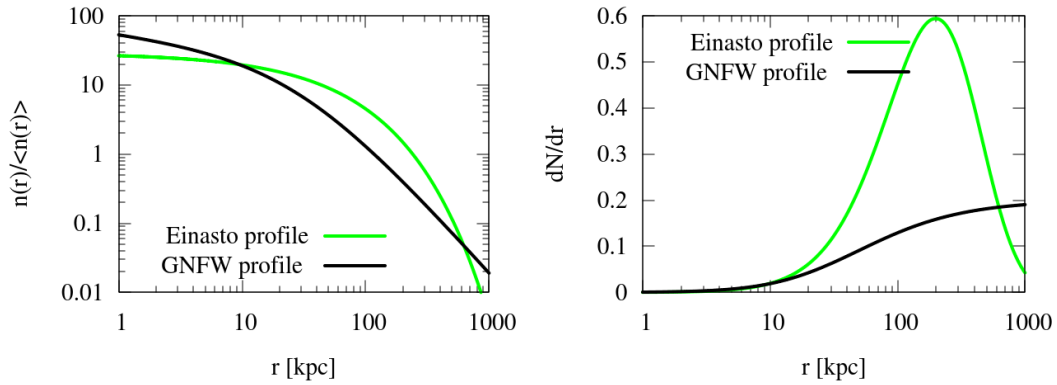

Figure 6. Comparison of two number density profiles, the Generalised NFW profile equation 3.2 (black) and the Einaso profile (green) equation 3.1 with the parameters seen in 3.1. Left panel shows the number density distribution, the Einaso is flatter at small radius where the GNFW is more extended at large radius. The right panel shows the fraction of source per radius range, most of sources are in the outer regions of the halo $r > 100kpc$ and it is even worst for the GNFW profile which remains extended farther than 1000kpc

3.2 Astrophysical sources profile

We decided to consider that some of our sources have an astrophysical origin, in particular those close to the galactic plane $b < 10°$ in order to make a fair comparison with the luminosity of M31, we cannot neglect their contribution to the total luminosity of the milky way, a good way to do is is to simulate an astrophysical component of gamma-ray emmiting sources.

The best candidates for the galactic unassociated sources are Millisecond Pulsars (ref all msp papers), we took a profile for the bulge and for the disk, and we considered a 10° box bulge (ref paper) where $n(r) \propto r^{-2.4}$ and a disk with $n(r) \propto \exp\left(-r^2/2\sigma_r^2\right) \exp\left(-z/z_r\right)$ where r and z are the galactic cylindrical coordinates, we took $\sigma_r = 5kpc$ and $z_r = 1kpc$ (check wich one is the right one (to myself)) [8],[9] [10]

We implement this profile for the low latitude sources of the 3FGL catalog, we justify this assumption with the latitude distribution of unassociated sources 3 where we see bunch of sources near the galactic plane where a DM subhalos population should be more isotropic.

4 M31 model

5 Luminosity calculation algorithme

5.1 Probabilité distribution

First, we need to calculate the probability for a source to be in a specific region of the galaxy, we will use the number density profiles seen in section 3.

The total number of subhalos is

$$N = \int n(\vec{r}) d^3\vec{r} \tag{5.1}$$

And in galactic coordinates:

$$N = \int n(r, b, l) r^2 dr cos(b) dbdl \tag{5.2}$$

where r is the distance from the galactic center, b and l respectively the galactic latitude and longitude.

The number of sources within two spheres of radius r et $r + dr$ and a solid angle $d\Omega = cos(b)dbdl$ is simply

$$dN = n(r, b, l)r^2 drcos(b)dbdl \tag{5.3}$$

If we assume an infinite precision on b,l values, the radial probability distribution for a source seen in (b,l) is then:

$$p_{b,l}(r) = \frac{dN}{N} = \frac{n(r, b, l)r^2}{\int_0^{dmax} n(r, b, l)r^2 dr} \tag{5.4}$$

Where d_{max} is the size of the galactic halo.

5.2 Frame origin change

So far we assumed the number distribution profile having a spherical symmetry, with an origin on the galactic center, let us consider now the Earth as an origin, we define caresian coordinates frame as : The Earth as the origin, the Oxy plan as the galactic plane, and the x axis defined by the line Earth-Galactic center. The Einasto number density profile becomes then :

$$n(x, y, z) = n_0 \exp(-\frac{2}{\alpha}((\frac{\sqrt{(x - d_\odot)^2 + y^2 + z^2}}{r_s})^\alpha - 1)) \tag{5.5}$$

Where $d_\odot$ is the distance of the sun from the center of the milky way.

We change again to galactic coordinates, $x = rcos(b)cos(l)$, $y = rcos(b)sin(l)$ and $z = rsin(b)$, we finally obtain:

$$n(r, b, l) = n_0 \exp(-\frac{2}{\alpha}((\frac{\sqrt{r^2 + d_\odot^2 - 2rd_\odot cos(b)cos(l)}}{r_s})^\alpha - 1)) \tag{5.6}$$

5.3 Algorithme

Let us assume we have for each region of the sky (b,l) a probability distribution, for a source to be under a radius r

$$P_{b,l}(r) = \int_0^r p(x, b, l)dx \tag{5.7}$$

For each source that we consider, we calculate its probability distribution, then we discretize the distance into a large number of small steps d_i which we associate the probability $P(d_i)$ for a source to have a distance from us smaller than d_i

The algorithme consists on randomly picking up values of probability (a number between 0 and 1) and finding the range of distance associated to this value.

We do this for each unassociated source, and calculate its luminosity.

$$L_j = 4\pi F_j d_j^2 \tag{5.8}$$

the total luminosity of unidentified sources is then simply

$$L = \sum_{j=1}^{N_{source}} L_j \tag{5.9}$$

We repeat this calculation many times and plot the histogram of results.

6 Results

6.1 Luminosity distribution

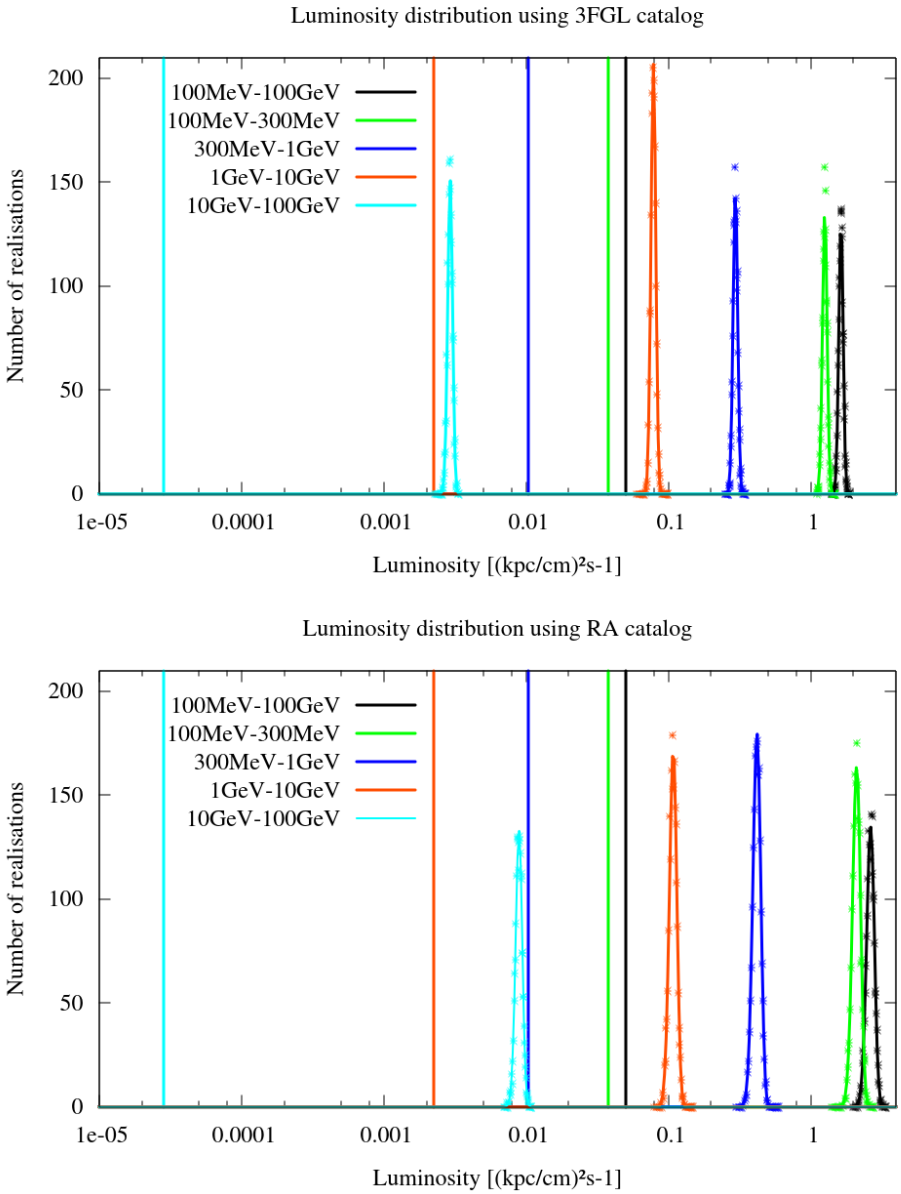

Figure 7. The luminosity distribution result for 2000 simulations of subhalos in the milky way dark matter halo (dots) with their gaussian fit for 5 different 8 sources after high latitude cut. bottom: using the RA catalog sources

6.1.1 3FGL

We obtain a strong constraint on the luminosity of subhalos, overlaping the M31 luminosity by more than 1 order of magnitude for the ranges 100MeV-300MeV, 300MeV-1GeV and 1GeV-10GeV, and by more than 3 orders of magnitude for the strongest constraint obtained for

the 10GeV-100GeV energy range,(ref fig res3fgl) result for 2000 montecarlos using the high latitude cutoff sample ($|b| > 1O°$).

6.1.2 Using the Refined Association catalog

The constraint obtained using the RA catalog is even stronger, nearly 2 orders of magnitude luminosity difference between M31 and our simulations for the ranges between 100MeV and 10 GeV, and almost 3 orders for the 10-100 GeV range,(figure res RA) this leads to the conclusion that a small number of the unassociated sources of both catalogs can be Dark Matter Subhalos.

6.2 Maximum number of detectable subhalos

We want now to quantify the number of subhalos that we can have in our galaxy without breaking the luminosity constraint of M31, we again use our two samples of sources and the same energy bands.

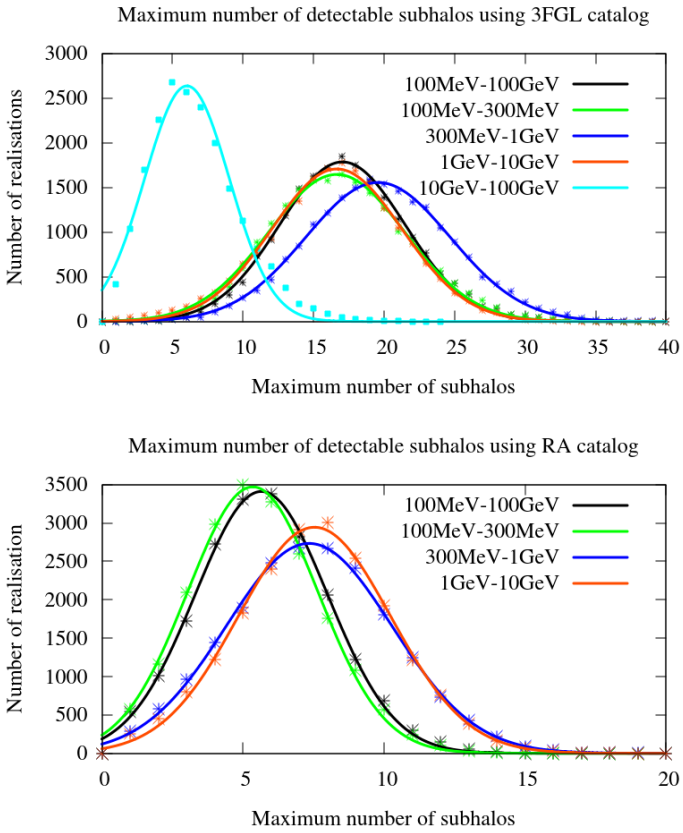

Figure 8. results from 20000 simulations showing the number of subhalo we can put in our galaxy before reaching the luminosity limit.top: using our sample from 3FGL catalog for all energy ranges. bottom: using the RA where for the 10GeV-100GeV the number was too small to be able to show it in this graph.

6.2.1 3FGL

The maximum number distribution for 3FGL sources is shown in (figure max3FGL), we can first say that these numbers are small when we compare to the number of sources, and as expected the strongest constraint is obtained for the higher energy range 10-100GeV around 5 subhalos, the larger number is obtained for the 300MeV to 1GeV range around 20 subhalos, and the others are around 17 maximum subhalos, the results are obtained for 20000 realisations, and the width of the gaussian is due to the difference in flux of the sources, since we take arbitrary ones, we reach the faster for luminous sources.

6.2.2 Refined Associations catalog

We do the same simulation using the RA catalog, and we unexpectedly find a different result, the maximu number of subhalos is lower than the previous case, around 5 and 7 (see figure maxRA) for the energy ranges between 100MeV to 10 GeV, and few ones for the 10-100GeV, which was too few to be plotted, thebibliography main reason for this difference is that RA sources (1FGL and 2FGL sources in general) are more luminous than 3FGL ones, so we reach the limit with a smaller number of subhalos.

7 Discussion

8 Conclusion

References

[1] Acero et al. F. Fermi Large Area Telescope Third Source Catalog. *Astrophys. J. Suppl.*, 2015.

[2] Bridget Bertoni, Dan Hooper, and Tim Linden. Examining The Fermi-LAT Third Source Catalog In Search Of Dark Matter Subhalos. 2015.

[3] Simon D. M. White and Carlos S. Frenk. Galaxy formation through hierarchical clustering. *Astrophys. J.*, 379:52–79, 1991.

[4] Jennifer M. Siegal-Gaskins, Vasiliki Pavlidou, A. V. Olinto, C. Brown, and Brian D. Fields. A luminosity constraint on the origin of unidentified high energy sources. *J. Phys.*, G36:055201, 2009.

[5] F. Massaro et al. Refining the Associations of the Fermi Large Area Telescope Source Catalogs. *Astrophys. J. Suppl.*, 217(1):2, 2015.

[6] Volker Springel, Jie Wang, Mark Vogelsberger, Aaron Ludlow, Adrian Jenkins, Amina Helmi, Julio F. Navarro, Carlos S. Frenk, and Simon D. M. White. The Aquarius Project: the subhalos of galactic halos. *Mon. Not. Roy. Astron. Soc.*, 391:1685–1711, 2008.

[7] Jurg Diemand, Michael Kuhlen, and Piero Madau. Formation and evolution of galaxy dark matter halos and their substructure. *Astrophys. J.*, 667:859–877, 2007.

[8] Qiang Yuan and Bing Zhang. Millisecond pulsar interpretation of the Galactic center gamma-ray excess. *JHEAp*, 3-4:1–8, 2014.

[9] Jovana Petrovic, Pasquale D. Serpico, and Gabrijela Zaharijas. Millisecond pulsars and the Galactic Center gamma-ray excess: the importance of luminosity function and secondary emission. *JCAP*, 1502(02):023, 2015.

[10] Tristan Grégoire and Jürgen Knödlseder. Constraining the Galactic millisecond pulsar population using Fermi Large Area Telescope. *Astron.Astrophys.*, 554:A62, 2013.